

# Journal of Materials Chemistry A

Accepted Manuscript



This is an *Accepted Manuscript*, which has been through the Royal Society of Chemistry peer review process and has been accepted for publication.

*Accepted Manuscripts* are published online shortly after acceptance, before technical editing, formatting and proof reading. Using this free service, authors can make their results available to the community, in citable form, before we publish the edited article. We will replace this *Accepted Manuscript* with the edited and formatted *Advance Article* as soon as it is available.

You can find more information about *Accepted Manuscripts* in the [Information for Authors](#).

Please note that technical editing may introduce minor changes to the text and/or graphics, which may alter content. The journal's standard [Terms & Conditions](#) and the [Ethical guidelines](#) still apply. In no event shall the Royal Society of Chemistry be held responsible for any errors or omissions in this *Accepted Manuscript* or any consequences arising from the use of any information it contains.

Cite this: DOI: 10.1039/c0xx00000x

www.rsc.org/xxxxxx

ARTICLE TYPE

## Selective Adsorption of CO<sub>2</sub>/CH<sub>4</sub>, CO<sub>2</sub>/N<sub>2</sub> Within a Charged Metal-Organic Framework

Lidan Kong,<sup>a</sup> Ruyi Zou,<sup>c</sup> Wenzhu Bi,<sup>c</sup> Ruiqin Zhong,<sup>b</sup> Weijun Mu,<sup>a</sup> Jia Liu,<sup>a</sup> Ray P.S. Han,<sup>a</sup> Ruqiang Zou<sup>a,\*</sup><sup>5</sup> Received (in XXX, XXX) XthXXXXXXXXXX 20XX, Accepted Xth XXXXXXXXXXXX 20XX

DOI: 10.1039/b000000x

Presented here is a new ultramicroporous metal-organic framework formulated as [Zn<sub>3</sub>L<sub>2</sub>(HCOO)<sub>1.5</sub>][(CH<sub>3</sub>)<sub>2</sub>NH<sub>2</sub>]<sub>1.5</sub>·xDMF, **1** (H<sub>3</sub>L = 9-(4-carboxy-phenyl)-9H-carbazole-3,6-dicarboxylic acid), consisting of anionic framework and two types of interlaced one-dimensional channels with 0.42 nm and 0.79 nm diameters respectively, in which the larger channels accommodate protonated dimethylamine as the counter cations. Gas sorption analysis of N<sub>2</sub>, CO<sub>2</sub> and CH<sub>4</sub> were investigated and the isotherms exhibit reversible thermodynamic behaviours without hysteresis desorption, evidencing the framework rigidity and permanent porosity of solvent-free **1**. The synergistic effect of the open ultramicropores and dimethylamine cations may lead to high efficiency separation of CO<sub>2</sub> from CH<sub>4</sub> and N<sub>2</sub>. According to the Toth model, the selectivity of CO<sub>2</sub>/CH<sub>4</sub> and CO<sub>2</sub>/N<sub>2</sub> were calculated to be 96 and 37, respectively. This effort will give rise to a new conception to tailor charged MOF for high efficiency CO<sub>2</sub> adsorption and separation.

### Introduction

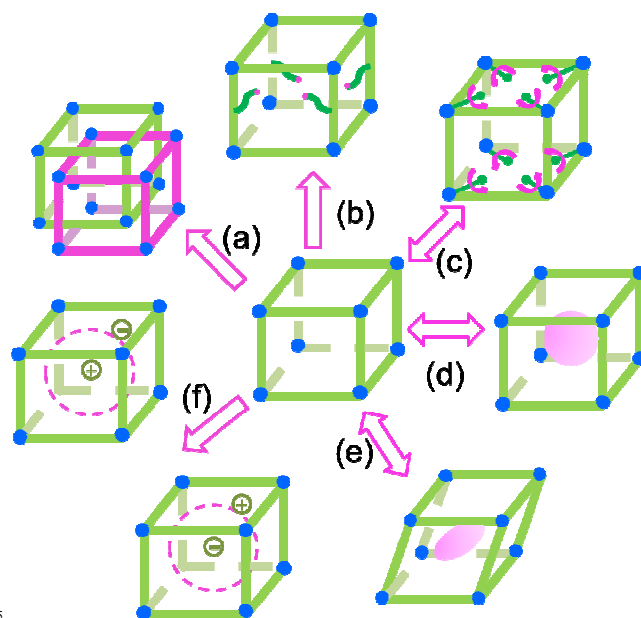
The separation of carbon dioxide from gas mixtures containing methane is particularly important in both scientific researches and industrial applications. Methane is the major component in many combustible gases, such as natural gas, biogas, coke oven gas, landfill gas, coal seam gas and straw syngas. Unfortunately, the coexistence of CO<sub>2</sub> in the fuel gases will not only lower their calorific values but also cause pipeline and equipment corrosion.<sup>1</sup> Besides, CO<sub>2</sub> is greenhouse gas which should be captured from releasing to the atmosphere. Technologies including cryogenic distillation, membrane separation, chemical scrubbing, and physical adsorption have been attempted to separate CO<sub>2</sub> from CH<sub>4</sub>.<sup>2</sup> Among these technologies, adsorption-based processes such as pressure-swing adsorption (PSA) and temperature-swing adsorption (TSA) are popular due to their low energy consumption and equipment cost.<sup>3</sup> Separation mechanisms of different systems can be divided into two types: equilibrium separation and kinetic separation. Equilibrium separation is based on equilibrium different adsorptive amount of gases. Kinetic separation is based on special steric effect, such as concentrating O<sub>2</sub> from air on carbon molecular sieve<sup>4</sup> or enrichment CH<sub>4</sub> from coal-bed methane on Clinoptilolites<sup>5</sup> and zeolite ETS.<sup>6</sup> However, in these techniques, the widely used porous absorbents, such as zeolites and active carbons, meanwhile bear the drawbacks of either relatively low selectivity or small capacity of CO<sub>2</sub>.<sup>7</sup>

Attractively, a new class of porous family, namely metal-organic frameworks (MOFs), has shined brilliantly on the aspect of CO<sub>2</sub> adsorption and separation in recent decades because of their structural diversities and numerous functionalities, such as

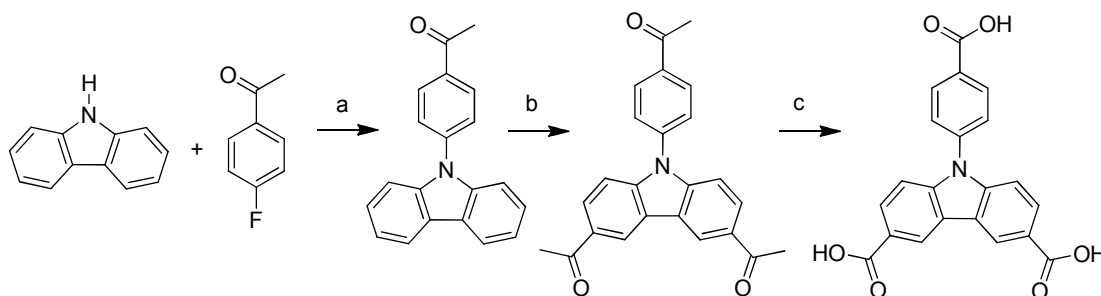
super-high surface area, tunable pore structures and functionalized pore walls and so on.<sup>8</sup> Since 2005, around 1400 papers relative to CO<sub>2</sub> adsorption and separation by MOFs have been published indexing from ISI web of science, among which ca. 60% focus on CO<sub>2</sub> separation (Graph S1). Generally, we can conceive six approaches to improve CO<sub>2</sub> separation as shown in Scheme 1, which may be suitable for other gas mixture separation: (I) Tuning of pore size contribution. Pore size contribution should be the most intuitive factor influencing the process of adsorptive separation. The predesigned pore sizes of MOFs can easily result in the controllable separation based on the difference of Van Der Waals diameters of the adsorbates. The separation mechanisms can be attributed to molecular sieving effect, dynamic adsorption effect or equilibrium adsorption effect. Recently, some new MOFs with ultramicroporous structures (< 7 Å) have promising properties for separating gases with similar molecular sizes,<sup>9</sup> in which interpenetration and catenation are frequently adopted to reduce the pore sizes of MOFs.<sup>10</sup> (II) Functionalization of pore walls. Modification of organic linkers on the pore walls is demonstrated to be another efficient method to enhance CO<sub>2</sub> uptakes and selectivity of the MOF materials, as well as reduction of pore sizes of MOF materials. The introduced functional groups and electron-rich atoms, including amidogen,<sup>11</sup> hydroxyl,<sup>12</sup> nitrogen atom<sup>13</sup> and fluorine atom,<sup>14</sup> exhibit remarkable intermolecular weak interaction with adsorbates by hydrogen bonding or electrostatic interactions. The functionalization can be easily realized through either directly self-assembly by using functional organic linkers or post-syntheses of MOF materials.<sup>15</sup> (III) Utilization of the vacancy of Lewis acid sites. The Lewis acid sites are the so-

called unsaturated coordinated metal sites within MOFs. These open metal sites are often occupied by some small volatile molecules, such as water, methanol,  $N,N'$ -dimethylformamide (DMF), etc., which can be easily removed or substituted without decomposition of the host frameworks of MOFs.<sup>16,17</sup> Recently, Long and his co-workers use ethanediamine to replace the bound solvent (DMF) within Cu-BTtri for  $CO_2$  adsorption. The result indicates that the ethanediamine modification can sharply enhance  $CO_2$  uptakes of Cu-BTtri under low pressure.<sup>18</sup> (IV) Modification of the large pores or open channels. The large pores or channels of MOFs often lead to poor confinement with small gas molecules, as reflected the low  $H_2$  and  $CO_2$  uptakes in MOF-177 compared with their analogies under low pressure.<sup>19</sup> However, modification of the large pores or channels by using functional small molecules, such as organic amine<sup>20</sup> and inorganic salts,<sup>21</sup> may be an efficient method to improve MOF performance. (V) Utilization of framework flexibility. It is noteworthy to note that the framework flexibility of MOFs can also be employed for the selection adsorption of  $CO_2$  since discovering the breathing effect of MIL-53 along with the change of pressure.<sup>22</sup> That is to say a contraction of the framework is induced by the strong interaction between polar functional groups and  $CO_2$  molecular, and the pores reopen with the increase of pressure. (VI) Introduction of electrostatic field. The design and synthesis of charged MOFs have received increasing attention.<sup>23-26</sup> The charged frameworks and counterion species may enhance the adsorbent-adsorbate interactions aroused by a strong electrostatic field in the cavity. Besides, the pore size and volume of framework are adjustable by the post modification of cation exchange, leading to ideal pore size for  $CO_2$  condensing.<sup>27-30</sup> A

molecular simulation result reported recently shows that the *rho* zeolite-like metal organic frameworks (*rho*-ZMOF), a series of anionic frameworks, exhibit excellent selectivity of  $CO_2$  from  $CH_4$ .<sup>27</sup>



**Scheme 1** Descriptions of the strategies to enhance  $CO_2/CH_4$  selectivity. (a) interpenetrate framework with ultramicropores; (b) functionalization of the pore environment; (c) utilization of open metal sites; (d) water modified large pores; (e) breathing effect of the framework; (f) charged framework.



**Scheme 2** Synthesis of  $H_3L$ . Reagent and conditions: (a)  $K_2CO_3$ , Cu, DMSO, 140 °C; (b)  $AlCl_3$ , acetyl chloride,  $CH_2Cl_2$ , RT; (c) Liquid Bromine, NaOH, p-dioxane/water, 60 °C.

It seems like that the strategy of charged framework is similar to the well-known post-synthetic modification, both of which can enhance  $CO_2$  capture by introducing extra zwitter-ions or functional groups into the framework. However, the post-synthetic work is not only tedious but also inefficient, for the small molecules which are expected to be incorporated into the inner part of the framework are more likely to accumulate on the surface of the material. By contrast, the synthesis of charged framework is much more convenient with the extra ions randomly and evenly distributed in the surface and internal of the framework. Herein, we report a novel ultramicroporous anionic MOF by reaction of zinc acetate dihydrate and a new N-contained tricarboxylate ligand under solvothermal condition, the formula of which was defined as  $[Zn_3L_2(HCOO)_{1.5}][(CH_3)_2NH_2]_{1.5} \cdot xDMF$ , **1** ( $H_3L$  = 9-(4-carboxy-phenyl)-9H-carbazole-3,6-dicarboxylic acid). The framework exhibits relatively high selectivity of  $CO_2$

over  $CH_4$  and  $N_2$ .

## Experimental Section

### Synthesis

The solvents and reagents for synthesis were commercially available and used without further treatment.  $H_3L$  was synthesized by classic Ullmann coupling procedure, followed by F-C acylation reaction and haloform reaction (Scheme 2).<sup>31</sup> In a typical preparation process of **1**,  $Zn(CH_3COO)_2 \cdot 2H_2O$  (0.1642 g, 0.75 mmol),  $H_3L$  (0.1891 g, 0.5 mmol), 80 mL DMF and 1 mL deionized water were placed in a 100 mL Teflon-lined steel autoclave. The autoclave was sealed, heated to 100 °C and kept at this temperature for two days, and then kept at 160 °C for another two days. After slowly cooling down to room temperature, pale yellow cubic crystals were obtained. The product was filtered out

and washed with DMF.

### Single-crystal X-ray crystallography

The crystal data was collected on Bruker APEXII CCD Detector single-crystal X-ray diffractometer at room temperature with Mo- $K\alpha$  radiation ( $\lambda = 0.71073 \text{ \AA}$ ).<sup>32</sup> The structures were solved by direct methods using the SHELXS program of the SHELXTL package and refined by full-matrix least-squares methods with SHELXL.<sup>33</sup> Zn atom in **1** was located from the E-maps and other non-hydrogen atoms were located in successive difference Fourier syntheses, which were refined with anisotropic thermal parameters on  $F_2$ . The hydrogen atoms of the ligands were generated theoretically onto the specific atoms and refined isotropically with fixed thermal factors. Part solvent molecules in the structure were randomly dispersed, and thus their positions were impossible to refine using conventional discrete-atom models. To resolve these issues, the contribution of solvent electron density was removed by the SQUEEZE routine in PLATON.<sup>34</sup> Crystal data for **1**: monoclinic, space group  $C2/c$  with  $a = 20.2644(6) \text{ \AA}$ ,  $b = 19.1216(7) \text{ \AA}$ ,  $c = 26.8248(9) \text{ \AA}$ ,  $\beta = 101.184(3)^\circ$ ,  $V = 10196.9(6) \text{ \AA}^3$ ,  $Z = 8$ ,  $\rho_{\text{calcd}} = 1.435 \text{ g cm}^{-3}$ . Least-squares refinement based on 8998 reflections with  $I > 2\sigma(I)$  and 611 parameters led to convergence, with a final  $R_1 = 0.0786$ ,  $R_w = 0.2165$ , and  $\text{GOF} = 1.021$ . CCDC 967970-967971 contains the supplementary crystallographic data for this paper. These data can be obtained free of charge via [www.ccdc.cam.ac.uk/conts/retrieving.html](http://www.ccdc.cam.ac.uk/conts/retrieving.html) (or from the Cambridge Crystallographic Data Centre, 12 Union Road, Cambridge CB21EZ, UK; fax: (+44) 1223-336-033; or [deposit@ccdc.cam.ac.uk](mailto:deposit@ccdc.cam.ac.uk)).

### Material Characterization

Powder X-ray diffraction (PXRD) were performed on a Rigaku Dmax/2400 X-ray diffractometer operating at 40 kV and 100 mA, using Cu- $K\alpha$  radiation ( $\lambda = 1.5406 \text{ \AA}$ ). Thermogravimetric analysis (TGA) was carried out under nitrogen atmosphere on a Q600 SDY TGA-DTA-DSC thermal analyzer from room temperature to  $600 \text{ }^\circ\text{C}$  with a heating rate of  $10 \text{ }^\circ\text{C/min}$ . Fourier Transform Infrared spectroscopy (FTIR) was recorded using an ECTOR22 Fourier transform infrared spectrometer between  $400$  and  $4000 \text{ cm}^{-1}$  in KBr pellets. Elemental analysis was performed on a Vario EL Elemental Analyzer. Cations exchange experiment was conducted by immersing **1a** in the saturated solution of  $\text{LiNO}_3$  in fresh DMF, at room temperature. The sample was soaked for 24 h before decanting the metal nitrate solution. The obtained sample was rinsed and washed with DMF for three times to remove free  $\text{LiNO}_3$ .

### Gas sorption measurements

Gas sorption data were collected by a QUANTACHROME AUTOSORB-IQ gas adsorption analyzer. Temperature of system was measured by a high precision thermometer with an accuracy of  $0.1 \text{ K}$  and the error of  $0.18\%$ . The relative error of the system is  $2.4\%$ . The raw samples were activated under vacuum at  $90 \text{ }^\circ\text{C}$  for 30 min and then at  $150 \text{ }^\circ\text{C}$  for 300 min to obtain solvent-free sample of **1a**. The  $\text{N}_2$  sorption isotherm was acquired in the pressure range of  $P/P_0$  from 0.01 to 0.99 at  $77 \text{ K}$  in a liquid nitrogen bath. The gas sorption experiments of  $\text{CO}_2$  and  $\text{CH}_4$  were conducted at  $273 \text{ K}$  in an ice-water bath.

## Results and discussion

### Synthesis

As well-known, factors such as pH value, solvent, reaction time, temperature, templates and so on, all play very important roles in constructing MOFs materials during solvothermal reactions.<sup>35</sup> In this work, we discovered that the amount of water contained in the system is one of vital factors that would influence the crystal growth of **1**. It should be noted that the high-temperature solvothermal reaction easily causes the hydrolysis of DMF,<sup>36</sup> and the hydrolyzates of formate and protonated dimethylamine ( $\text{DMA}^+$ ) may take participate in the construction of MOF structure. Actually, quite a few charged MOFs, especially anionic ones, have in situ formed  $\text{DMA}^+$  cations trapped in their pores or channels as counterions.<sup>23,25,27,36-43</sup> In this work, the existence of trace water can impact the hydrolysis of DMF and precipitation of **1**. Excess water may result in the formation of zinc formate byproducts.<sup>36</sup> Without water, only gel-like species was obtained at the bottom of clarified liquid. On the other hand, temperature also plays an important role to obtain high purity product. Since the mixture of zinc acetate,  $\text{H}_3\text{L}$  and DMF turns out white slurry at room temperature, it was maintained at  $100 \text{ }^\circ\text{C}$  for one day to become clear solution, after which the temperature was increased to  $160 \text{ }^\circ\text{C}$  for crystal growth. PXRD patterns of both the original and the solvent-free samples are consistent with the simulated one from single crystal structure (Fig. S12), indicating the high purity and the framework stability of **1**.

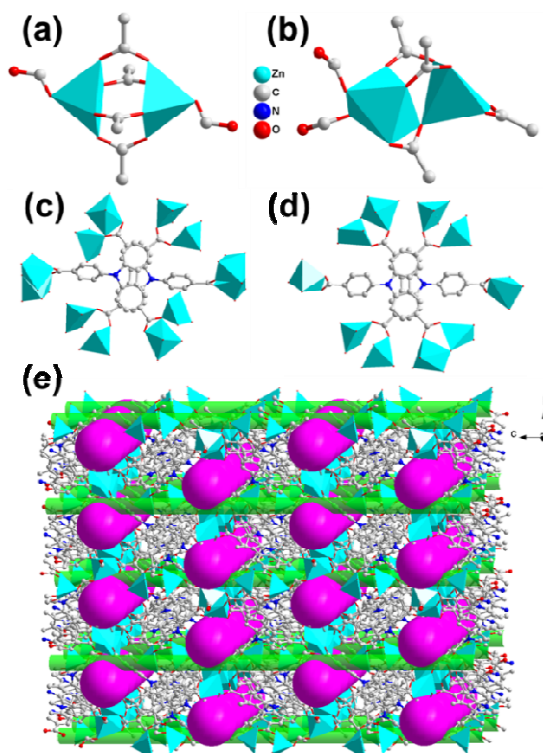


**Fig. 1** View of (a) coordination environment of symmetric paddle-wheel binuclear cluster; (b) asymmetric binuclear metal cluster; (c) ligand pair stacking by intermolecular  $\pi$ - $\pi$  interaction as a 6-connected node with a torsional angle of  $64.3(4)$ ; (d) ligand pair with a torsional angle of  $54.6(4)$ ; (e) three-dimensional porous framework with two types of crossed channels. Pink: large channels blocked by  $\text{DMA}^+$  along a direction and Green: small hollow channels along  $c$  direction.

### Crystal structure description

X-Ray crystallographic analysis indicates that **1** crystallizes in a monoclinic  $C2/c$  space group, consisting of anionic  $[Zn_6L_4(HCOO)_3]^{3-}$  framework and  $DMA^+$  cations. The host framework is composed of three crystallographic independent Zn(II) coordinated to two **L** ligands and one and a half formate anions in an asymmetric unit. Two symmetric Zn(1) ions are coupled into a paddle-wheel building block by four carboxylate groups from four separate **L** ligands (Fig. 1a). Two terminal coordinate sites of the dinuclear cluster are occupied by two bridge formate anions. The Zn-Zn separation of 2.961(1) Å is a little longer than that of the reported Cu-Cu paddle wheel clusters.<sup>44</sup> Zn(2) adopts a slightly distorted octahedral coordination fashion with two *syn-syn* bridging formates and three carboxylate groups in *syn-syn* bridging and  $\eta$ -O, O'- $\mu$ -O, O modes, while Zn(3) has a five coordinate configuration with four carboxylate groups in *syn-syn* bridging,  $\eta_2$ , and  $\eta$ -O, O'- $\mu$ -O, O

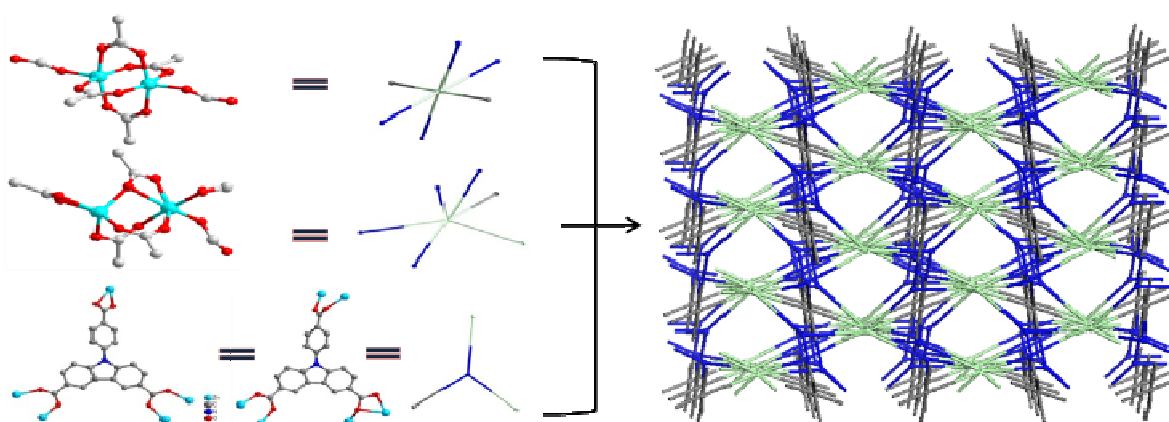


Fig. 2 Topological graph of the anion framework of **1a**.

To better understand such a complicated structure, the topology of the anion framework of **1a** was studied by using Topos 4.0 software.<sup>46,47</sup> The network topology is based on 3-connected(3-c) ligands and two types of 6-connected (6-c) metal clusters. The structure has a 3,6-connected (3,6-c) net with stoichiometry  $(3-c)_4(6-c)_3$  (Fig. 2). Therefore, **1a** self-assembles into a new three-dimensional net with the point Schläfli symbol of  $\{5;6^2\}_2\{5^2;6\}_2\{5^3;6^4;7^6;8;9\}\{5^5;6^4;7^5;9\}_2$ .

### Properties characterization

Thermogravimetric analysis of as synthesized **1** shows a significant decline before 200 °C, indicating the loss of solvents (Fig. S11). The subsequent platform implies that **1** could keep stable below 400 °C, after which the framework collapsed according to the sharp decline of the curve. A detailed investigation of TG curve of **1a** was then conducted. The slight decline before 250 °C is attributed to the loss of re-adsorbed water when exposed to atmosphere air. The results are further confirmed by elemental analysis experiment, implying **1a** formulate as  $[Zn_3L_2(HCOO)_{1.5}][(CH_3)_2NH_2]_{1.5} \cdot 3H_2O$  (observed (wt%): C 49.05, H 3.45, N 4.29; calculate (wt%): C 49.40, H 3.50, N 4.34). Theoretical weight loss for the coordinated water is 4.78%, which is corresponding to the TGA result (4.11%). The subsequent weight loss of 7.01% from 250 to 400 °C is attributed to the decomposition of  $DMA^+$  (theoretical weight loss of 6.11%),

respectively. The Zn(2) and Zn(3) are linked by three bridging carboxylate to lead a dinuclear clusters with the closest separation of 3.244(1) Å (Fig. S1). All Zn-O bond lengths fall into the normal range of 1.997-2.043 Å. Furthermore, the two types of dinuclear clusters are linked together by bridging formates in 1:2 stoichiometric ratio.

The two crystallographic dependent **L** ligands coordinate five and six separate metal centers to lead a three-dimensional network with two types of molecular channels with the dimension of  $4.0 \times 4.8$  Å<sup>2</sup> and  $4.2 \times 8.0$  Å<sup>2</sup>, respectively. The corresponding protonated  $DMA^+$  are trapped in the large channels (Fig. 1e). And a detailed research of the location of  $DMA^+$  demonstrates that the cations are connected to the host framework by hydrogen bond (Fig. S2), which further infers the intrinsic stability of **1**. Notably, the centroid-to-centroid separations of the carbazole rings of two straggled **L** ligand pairs fall into the range of 3.243-3.573 Å (Fig. S3), implying strong intermolecular  $\pi$ - $\pi$  stacking interactions.<sup>45</sup>

which was reported to happen at around 300 °C.<sup>38,48</sup> It appears as a smooth slope rather than a step, which might be resulted from the hydrogen bond between  $DMA^+$  and the framework.

Cations exchange experiment indicates that  $DMA^+$  in the framework can't be exchanged at room temperature, as proven by elemental analysis (Table S3). We attributed this to the existence of hydrogen bond.

As seen in the PXRD pattern (Fig.S12), the peak positions of **1a** are in good agreement with that of the simulated patterns, indicating that **1** retains its framework integrity after the removal of the guest molecule.

In the FTIR spectra of **1a** (Fig. S9, S10), the C-O vibration peak of carboxyl groups occurs at  $1657$  cm<sup>-1</sup>, which is red-shifted compared with that of the free carboxyl groups of  $H_3L$ . This shift was ascribed to the coordination of oxide atoms of carboxyl groups to metal ions. Another evidence of the formation of Zn-O coordination bonds is the sharply weakened peaks in the range of  $3200$ - $2500$  cm<sup>-1</sup>, which is corresponded to the binary associated hydroxyl. Specially, the peaks at  $3430$  and  $1476$  cm<sup>-1</sup> correspond to the stretching vibration of N-H and C-N bonds in  $DMA^+$ , respectively, which further demonstrates its existence inside the framework.

### Gas sorption properties

The  $N_2$  sorption isotherm of **1a** at 77 K exhibits a typical Type-I

sorption behavior and reversible adsorption/desorption property with the largest uptake amount of  $153.4 \text{ cm}^3 \text{ g}^{-1}$  (Fig. 2), demonstrating the permanent porosity of the framework. Dubinin-Radushkevich (DR) equation<sup>49</sup> gives the pore volume of  $0.237 \text{ cm}^3 \text{ g}^{-1}$ , which is comparable to the theoretical value of  $0.241 \text{ cm}^3 \text{ g}^{-1}$  calculated by PLATON.<sup>34</sup> Moreover, the analysis of pore width distribution by the method of Horvath Kawazoe (HK) shows that there are two types of ultramicropores with a dimension of 0.423 and 0.795 nm respectively, which is in good agreement with the crystal structure refinement result. The specific surface area is calculated to be  $569.5 \text{ m}^2 \text{ g}^{-1}$  using Brunauer-Emmett-Teller (BET) model, which is lower than that of other ultramicroporous frameworks with similar pore size.<sup>50</sup> One possible reason is that  $\text{DMA}^+$  cations blocked in the large channels prevent the entrance of  $\text{N}_2$  molecules, leading to the inner part of the channel unavailable. Moreover, this statement can also be used to illustrate the fact that the peak at 0.795 nm is much weaker than that at 0.423 nm in the figure of pore size distribution.

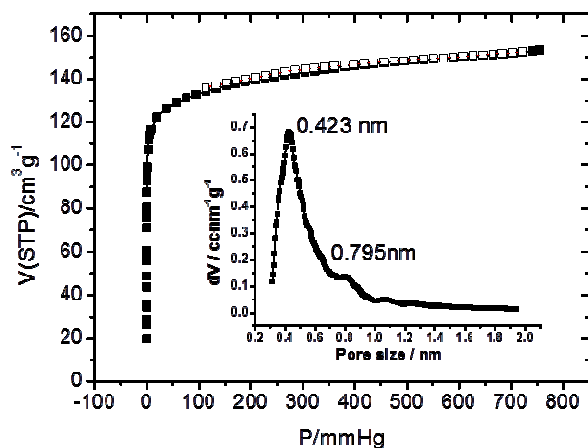


Fig. 3  $\text{N}_2$  sorption isotherms at 77K. Filled shapes: adsorption. Open shapes: desorption. Inset: pore size distribution calculated by HK method.

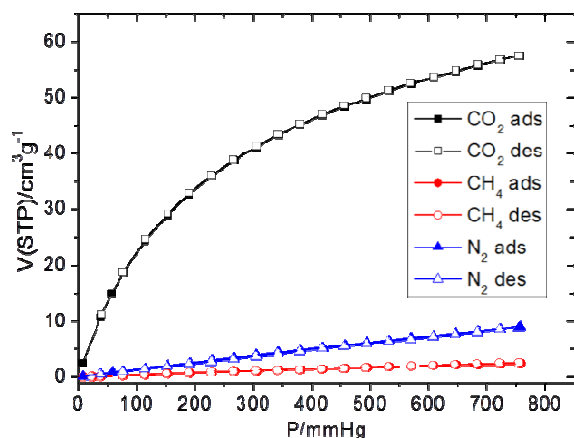


Fig. 4  $\text{CO}_2$ ,  $\text{N}_2$  and  $\text{CH}_4$  sorption isotherms of compound **1a** at 273K. Filled shapes: adsorption. Open shapes: desorption.

Table 1 Selectivity of  $\text{CO}_2/\text{CH}_4$  and  $\text{CO}_2/\text{N}_2$  at 273K.

Calculation methods	$\text{CO}_2/\text{CH}_4$	$\text{CO}_2/\text{N}_2$
Langmuir model	85	25
Toth model	96	37
Initial slope ratio	64	17
Weight uptake ratio	64	10
Average	77.2	22.2
IAST	$87^a$ , 1744 <sup>b</sup>	24

<sup>a</sup> $2.6 \times 10^{-5}$  bar, 50/50; <sup>b</sup> 1bar, 50/50.

Since the framework of **1a** has permanent porosity and the seemingly like pore controlled sorption property, its potential application on selective gas sorption can be expected. Here we studied the sorption behavior of  $\text{CO}_2$ ,  $\text{N}_2$  and  $\text{CH}_4$  at 273 K (Fig. 4). The largest uptake amount of  $\text{CO}_2$  is  $57.5 \text{ cm}^3 \text{ g}^{-1}$  ( $2.57 \text{ mmol g}^{-1}$ ) at 1 atm, while that of  $\text{N}_2$  ( $8.93 \text{ cm}^3 \text{ g}^{-1}$ ) and  $\text{CH}_4$  ( $2.48 \text{ cm}^3 \text{ g}^{-1}$ ) is quite lower in the same condition. Here, the adsorption amount of  $\text{N}_2$  is abnormally higher than that of  $\text{CH}_4$ , which can be reasonably ascribed to the molecular sieve effect,<sup>51</sup> for the diameter of  $\text{CH}_4$  (3.76 Å) molecular is a little larger than that of  $\text{N}_2$  (3.646 Å).

The significant difference of uptake amounts makes **1a** great promise for the application of gas separation. Herein, we adopt four general methods: weight uptake ratio,<sup>52</sup> initial slope ratio,<sup>53</sup> dual-site Langmuir isotherm model and Toth model,<sup>54</sup> to calculate the selectivity (Table 1). Average selectivity of  $\text{CO}_2/\text{CH}_4$  and  $\text{CO}_2/\text{N}_2$  were calculated to be 77.2 and 22.2 respectively. To further explore the gas separation properties of **1a**, Ideal Adsorbed Solution Theory (IAST) method was used to calculate the selectivities (see Supporting Information).<sup>55, 56</sup> For an equimolar mixture of  $\text{CO}_2$  and  $\text{CH}_4$ , the selectivity was calculated to be 87 at very low pressure ( $< 0.1 \text{ mmHg}$ , Fig. S19), which matches well with the other calculation results. Interestingly, the selectivity increases sharply as the increase of pressure, which is quite different from other MOFs. The selectivity of  $\text{CO}_2/\text{CH}_4$  reaches up to 1744 at atmosphere pressure, which is much higher than the ever reported charged and neutral MOFs listed in Table 2.<sup>9,17,27-29,39,57-65</sup> The satisfying high selectivity of  $\text{CO}_2$  was attributed to the synergistic effect of pore size effect and the enhanced host-guest interaction caused by the immobile  $\text{DMA}^+$ . It is well-known that the kinetic diameter of  $\text{CH}_4$  and  $\text{N}_2$  is slightly larger than that of  $\text{CO}_2$  (3.30 Å), and the similar size is one of the most important factor that hinders their separation. In the framework of **1a**, there are channels with different sizes: 0.423 and 0.795 nm. It is easy to understand that  $\text{CH}_4$  and  $\text{N}_2$  molecules are more difficult to pass through the small channels. Meanwhile, with  $\text{DMA}^+$  inside, the remained pore space of large channels becomes too small to accommodate  $\text{CH}_4$  and  $\text{N}_2$  molecules. In addition, the existence of  $\text{DMA}^+$  enhances the interaction between the host compound and  $\text{CO}_2$  molecules. When flowing through small channels,  $\text{CO}_2$  molecules interact strongly with  $\text{DMA}^+$  ions blocking in the intercrossed large channels, thus the adsorption was enhanced. In contrast, the near-linear adsorption isotherms of  $\text{CH}_4$  and  $\text{N}_2$  are indicative of their low affinity to the charged framework, which can be expected from its relatively low polarizability.

In the three gas sorption isotherms of  $\text{N}_2$ ,  $\text{CO}_2$ ,  $\text{CH}_4$ , desorption curves almost completely coincide with corresponding adsorption curves. Without hysteretic desorption behaviour, the framework

Cite this: DOI: 10.1039/c0xx00000x

www.rsc.org/xxxxxx

## ARTICLE TYPE

is bound to be unreformed and the pore structure should be maintained during the sorption test, which further confirms the rigidity of **1**. Therefore, its application in gas storage and

separation, especially CO<sub>2</sub>/CH<sub>4</sub> separation for natural gas purification, can be energetically expected.

**Table 2** CO<sub>2</sub> separation properties of some MOFs.

MOFs	Selectivity		C <sub>CO<sub>2</sub></sub> /%	E/S	T/K	P/bar	Ref
	CO <sub>2</sub> /CH <sub>4</sub>	CO <sub>2</sub> /N <sub>2</sub>					
Mg(dobdc) <sub>2</sub> /Mg-MOF-74	283	–	–	E	298	1	17
	–	800	–	–	313	1	58
rho-ZMOF	80	–	50	S	298	1	27
	–	500	15	S	298	1	27
rho-ZMOF	–	22.6	–	E	298	1	29
sod-ZMOF	–	20.4	–	E	298	1	29
ZIF-78	10.6	50.1	50	E	298	1	57
Zn <sub>2</sub> (bpdcc) <sub>2</sub> (bpee)(DMF) <sub>2</sub>	257	–	–	E	298	0.16	59
	–	116	–	E	298	1	59
SNU-151/[Zn <sub>5</sub> (NTN) <sub>4</sub> (DEF) <sub>2</sub> ][NH <sub>2</sub> (C <sub>2</sub> H <sub>5</sub> ) <sub>2</sub> ] <sub>2</sub>	7.2	–	50	E	298	1	39
	–	30	15	E	298	1	39
SIFSIX-2-Cu-i	33/51	–	50	E	298	1	9
	–	140/72	10	E	298	1	9
SIFXIX-3-Zn	231/305	–	50	E	298	1	9
	–	1818/1700	10	E	298	1	9
100Ksod-ZMOF	–	172.74	–	S	308	10	28
UTSA-16/[K(H <sub>2</sub> O) <sub>2</sub> Co <sub>3</sub> (cit)(Hcit)]	29.8	–	50	E	296	2	60
	–	314.7	15	E	296	2	60
mmenCuBTri	–	329.0	15	E	296	2	60
Compound 1	1744	–	50	S	273	1	This work
	–	25	15	S	273	1	This work
azo-COP-3	–	288.1,	15	S	323	1	61
polyamine-tethered PPNS	–	442	15	S	295	1	62
POP(2)	–	155	10	S	298	1	63
FCTF-1-600	–	19/152	10	S/E	298	1	64

C<sub>CO<sub>2</sub></sub>/%: Concentration of CO<sub>2</sub>; E/S: experiment/simulation**Conclusions**

<sup>10</sup> In conclusion, a novel charged MOF was prepared and exhibited relatively potential high selectivity of CO<sub>2</sub> over CH<sub>4</sub> and N<sub>2</sub>. In addition to the pore size effect, extraframework DMA<sup>+</sup> may largely enhance the host-guest interaction during the adsorption of CO<sub>2</sub>. The results reveal that anionic frameworks with

<sup>15</sup> appropriate pore size are excellent candidates for gas separation. Further study is expected to design and synthesize new type of charged framework with in situ formed counter ions. With one kind of species randomly distributed into another, charged MOF can be considered as “composite material”, and its “one-pot” <sup>20</sup> method is inspirational to synthetic methodology.

## Acknowledgements

This work was supported by National Natural Science Foundation of China 11175006, 51322205 and 21371014, the Ministry of education program for New Century Excellent Talents of China (NCET-11-0027), and Singapore-Peking University SPURc program.

## Notes and References

<sup>a</sup> College of Engineering, Peking University, Beijing 100871, China. Fax: +86-10-82529010; Tel: +86-10-82529045; E-mail: rzou@pku.edu.cn.

<sup>b</sup> State Key Laboratory of Heavy Oil Processing, China University of Petroleum, Beijing, 102249, China

<sup>c</sup> College of Chemistry and Molecule Engineering, Zhengzhou University, Zhengzhou 450001, Henan, China

† Electronic Supplementary Information (ESI) available: ISI stastical result about CO<sub>2</sub> adsorption and separation (Graph S1), Crystallographic data and structural refinement summary for compound **1** (Table S1), selected bond distances and angles for compound **1** (Table S2), crystal structure description (Fig. S1-S8), FTIR spectra (Fig. S9 and S10), TGA curves (Fig. S11), XRD data (Fig. S12), Langmuir fitting results for calculation of selectivity (Fig. S13-15), Toth fitting results for calculation of selectivity (Fig. S16-18), calculation result of selectivity by IAST method (Fig. S19). CCDC reference numbers CCDC 967970-967971. For ESI and catalographic data in CIF or other electronic format see DOI: 10.1039/b000000x/.

- R. W. Baker, *Ind. Eng. Chem. Res.*, 2002, **41**, 1393-1411.
- D. M. D'Alessandro, B. Smit and J. R. Long, *Angew. Chem. Int. Ed.*, 2010, **49**, 6058-6082.
- G. D. Pirngruber, L. Hamon, S. Bourrelly, P. L. Llewellyn, E. Lenoir, V. Guillerm, C. Serre and T. Devic, *Chemsuschem*, 2012, **5**, 762-776.
- T. R. Gaffney, *Curr. Opin. Solid State Mater. Sci.*, 1996, **1**, 69-75.
- A. Jayaraman, A. J. Hernandez-Maldonado, R. T. Yang, D. Chinn, C. L. Munson and D. H. Mohr, *Chem. Eng. Sci.*, 2004, **59**, 2407-2417.
- A. Ansón, S. M. Kuznicki, T. Kuznicki, T. Hastrup, Y. Wang, C. C. H. Lin, J. A. Sawada, E. M. Eyring and D. Hunter, *Micropor. Mesopor. Mater.*, 2008, **109**, 577-580.
- J. McEwen, J. D. Hayman and A. O. Yazaydin, *Chem. Phys.*, 2013, **412**, 72-76.
- K. Sumida, D. L. Rogow, J. A. Mason, T. M. McDonald, E. D. Bloch, Z. R. Herm, T.-H. Bae and J. R. Long, *Chem. Rev.*, 2012, **112**, 724-781.
- P. Nugent, Y. Belmabkhout, S. D. Burd, A. J. Cairns, R. Luebke, K. Forrest, T. Pham, S. Ma, B. Space, L. Wojtas, M. Eddaoudi and M. J. Zaworotko, *Nature*, 2013, **495**, 80-84.
- B. Liu, L. X. Tang, Y. H. Lian, Z. Li, C. Y. Sun and G. J. Chen, *Acta Chim. Sinica*, 2013, **71**, 920-928.
- S. Vaesen, V. Guillerm, Q. Y. Yang, A. D. Wiersum, B. Marszalek, B. Gil, A. Vimont, M. Daturi, T. Devic, P. L. Llewellyn, C. Serre, G. Maurin and G. De Weireld, *Chem. Commun.*, 2013, **49**, 10082-10084.
- I. Spanopoulos, P. Xydias, C. D. Malliakas and P. N. Trikalitis, *Inorg. Chem.*, 2013, **52**, 855-862.
- P. Z. Li and Y. L. Zhao, *Chem. Asian J.*, 2013, **8**, 1680-1691.
- D.-X. Xue, A. J. Cairns, Y. Belmabkhout, L. Wojtas, Y. Liu, M. H. Alkordi and M. Eddaoudi, *J. Am. Chem. Soc.*, 2013, **135**, 7660-7667.
- Q. J. Yan, Y. C. Lin, P. Y. Wu, L. Zhao, L. J. Cao, L. M. Peng, C. L. Kong and L. Chen, *Chempluschem*, 2013, **78**, 86-91.
- H. Xu, Y. B. He, Z. J. Zhang, S. C. Xiang, J. F. Cai, Y. J. Cui, Y. Yang, G. D. Qian and B. L. Chen, *J. Mater. Chem. A*, 2013, **1**, 77-81.
- Z. Bao, L. Yu, Q. Ren, X. Lu and S. Deng, *J. Colloid Interface Sci.*, 2011, **353**, 549-556.
- A. Demessence, D. M. D'Alessandro, M. L. Foo and J. R. Long, *J. Am. Chem. Soc.*, 2009, **131**, 8784-8786.
- J. L. C. Rowsell, A. R. Millward, K. S. Park and O. M. Yaghi, *J. Am. Chem. Soc.*, 2004, **126**, 5666-5667.
- T. M. McDonald, W. R. Lee, J. A. Mason, B. M. Wiers, C. S. Hong and J. R. Long, *J. Am. Chem. Soc.*, 2012, **134**, 7056-7065.
- Z. J. Zhang, W. Y. Gao, L. Wojtas, S. Q. Ma, M. Eddaoudi and M. J. Zaworotko, *Angew. Chem. Int. Ed.*, 2012, **51**, 9330-9334.
- B. Zornoza, A. Martinez-Joaristi, P. Serra-Crespo, C. Tellez, J. Coronas, J. Gascon and F. Kapteijn, *Chem. Commun.*, 2011, **47**, 9522-9524.
- A. K. Chaudhari, S. Mukherjee, S. S. Nagarkar, B. Joarder and S. K. Ghosh, *CrystEngComm*, 2013, **15**, 9465-9471.
- P. He, H. Liu, Y. F. Li, Z. G. Lei, S. P. Huang, P. Wang and H. P. Tian, *Mol. Simulat.*, 2012, **38**, 72-83.
- T. Li and N. L. Rosi, *Chem. Commun.*, 2013, **49**, 11385-11387.
- R. Babarao, M. Eddaoudi and J. W. Jiang, *Langmuir*, 2010, **26**, 11196-11203.
- R. Babarao and J. W. Jiang, *J. Am. Chem. Soc.*, 2009, **131**, 11417-11425.
- B. Demir and M. G. Ahunbay, *J. Phys. Chem. C*, 2013, **117**, 15647-15658.
- C. Chen, J. Kim, D. A. Yang and W. S. Ahn, *Chem. Eng. J.*, 2011, **168**, 1134-1139.
- Y. F. Chen, A. Nalaparaju, M. Eddaoudi and J. W. Jiang, *Langmuir*, 2012, **28**, 3903-3910.
- S. B. Choi, M. J. Seo, M. Cho, Y. Kim, M. K. Jin, D.-Y. Jung, J.-S. Choi, W.-S. Ahn, J. L. C. Rowsell and J. Kim, *Cryst. Growth Des.*, 2007, **7**, 2290-2293.
- H. T. Program for Absorption Correction, Rigaku Corporation, Tokyo, Japan, 1995.
- G. M. Sheldrick, *SHELXTL NT, Program for Solution and Refinement of Crystal Structures, Version 5.1*, University of Göttingen, Göttingen, Germany, 1997.
- A. L. Spek, *PLATON, A Multipurpose Crystallographic Tool*, Utrecht University, Utrecht, The Netherlands, 2001.
- N. Stock and S. Biswas, *Chem. Rev.*, 2012, **112**, 933-969.
- A. D. Burrows, K. Cassar, R. M. W. Friend, M. F. Mahon, S. P. Rigby and J. E. Warren, *CrystEngComm*, 2005, **7**, 548-550.
- E. Q. Procopio, F. Linares, C. Montoro, V. Colombo, A. Maspero, E. Barea and J. A. R. Navarro, *Angew. Chem. Int. Ed.*, 2010, **49**, 7308-7311.
- Y.-X. Tan, Y.-P. He and J. Zhang, *Chem. Commun.*, 2011, **47**, 10647.
- M.-H. Choi, H. J. Park, D. H. Hong and M. P. Suh, *Chem. Eur. J.*, 2013, **19**, 17432-17438.
- Q.-G. Zhai, Q. Lin, T. Wu, L. Wang, S.-T. Zheng, X. Bu and P. Feng, *Chem. Mater.*, 2012, **24**, 2624-2626.
- S. M. Chen, J. Zhang, T. Wu, P. Y. Feng and X. H. Bu, *J. Am. Chem. Soc.*, 2009, **131**, 16027-16029.
- D. Peralta, G. Chaplais, A. Simon-Masseron, K. Barthelet, C. Chizallet, A. A. Quoineaud and G. D. Pirngruber, *J. Am. Chem. Soc.*, 2012, **134**, 8115-8126.
- Y. Liu, V. C. Kravtsov, R. Larsen and M. Eddaoudi, *Chem. Commun.*, 2006, 1488-1490.

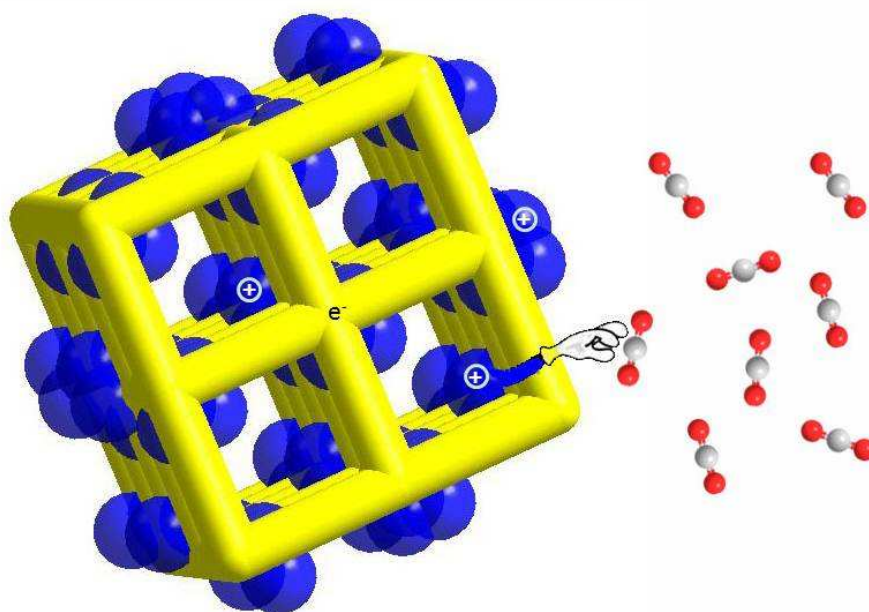


44. R.-Q. Zou, H. Sakurai, S. Han, R.-Q. Zhong and Q. Xu, *J. Am. Chem. Soc.*, 2007, **129**, 8402-8403.
45. R. Zou, A. I. Abdel-Fattah, H. Xu, A. K. Burrell, T. E. Larson, T. M. McCleskey, Q. Wei, M. T. Janicke, D. D. Hickmott, T. V. Timofeeva  
5 and Y. Zhao, *Cryst. Growth Des.*, 2010, **10**, 1301-1306.
46. M. O'Keeffe, M. A. Peskov, S. J. Ramsden and O. M. Yaghi, *Accounts. Chem. Res.*, 2008, **41**, 1782-1789.
47. S. R. Batten, N. R. Champness, X.-M. Chen, J. Garcia-Martinez, S. Kitagawa, L. Öhrström, M. O'Keeffe, M. Paik Suh and J. Reedijk,  
10 *Pure Appl. Chem.*, 2013, **85**, 1715-1724.
48. M. E. Medina, Y. Dumont, J.-M. Grenèche and F. Millange, *Chem. Commun.*, 2010, **46**, 7987-7989.
49. A. Gil and P. Grange, *Colloids Surf. A*, 1996, **113**, 39-50.
50. Z. Lin, R. Zou, J. Liang, W. Xia, D. Xia, Y. Wang, J. Lin, T. Hu, Q.  
15 Chen, X. Wang, Y. Zhao and A. K. Burrell, *J. Mater. Chem.*, 2012, **22**, 7813-7818.
51. S. Cavenati, C. A. Grande and A. E. Rodrigues, *J. Chem. Eng. Data*, 2004, **49**, 1095-1101.
52. T. K. Kim and M. P. Suh, *Chem. Commun.*, 2011, **47**, 4258-4260.
- 20 53. R. Banerjee, H. Furukawa, D. Britt, C. Knobler, M. O'Keeffe and O. M. Yaghi, *J. Am. Chem. Soc.*, 2009, **131**, 3875-3877.
54. Z. X. Chen, S. C. Xiang, H. D. Arman, J. U. Monda, P. Li, D. Y. Zhao and B. L. Chen, *Inorg. Chem.*, 2011, **50**, 3442-3446.
55. A. L. Myers and J. M. Prausnitz, *AIChE. J.*, 1965, **11**, 121-127.
- 25 56. B. P. Bering and V. V. Serpenski, *Zhur. Fiz. Khim.*, 1952, **26**, 253-269.
57. A. Phan, C. J. Doonan, F. J. Uribe-Romo, C. B. Knobler, M. O'Keeffe and O. M. Yaghi, *Accounts. Chem. Res.*, 2009, **43**, 58-67.
58. Z. R. Herm, J. A. Swisher, B. Smit, R. Krishna and J. R. Long, *J. Am.*  
30 *Chem. Soc.*, 2011, **133**, 5664-5667.
59. H. Wu, R. S. Reali, D. A. Smith, M. C. Trachtenberg and J. Li, *Chem. Eur J.*, 2010, **16**, 13951-13954.
60. S. Xiang, Y. He, Z. Zhang, H. Wu, W. Zhou, R. Krishna and B. Chen, *Nat. Commun*, 2012, **3**, 954-963.
- 35 61. H. A. Patel, S. H. Je, J. Park, D. P. Chen, Y. Jung, C. T. Yavuz and A. Coskun, *Nat. Commun.*, 2013, **4**, 1357.
62. W. Lu, J. P. Sculley, D. Yuan, R. Krishna, Z. Wei and H. C. Zhou, *Angew. Chem., Int. Ed.*, 2012, **51**, 7480-7484.
63. V. Guillermin, L. J. Weselinski, M. Alkordi, M. I. Mohideen, Y.  
40 Belmabkhout, A. J. Cairns and M. Eddaoudi, *Chem. Commun.*, 2014, **50**, 1937-1940.
64. Y. Zhao, K. X. Yao, B. Teng, T. Zhang and Y. Han, *Energy Environ. Sci.*, 2013, **6**, 3684-3692.
- 45 65. J. Liu, P. K. Thallapally, B. P. McGrail, Daryl R. Brown and J. Liu, *Chem. Soc. Rev.*, 2012, **41**, 2308-2322.

## Graphical Abstract

## Selective Adsorption of CO<sub>2</sub>/CH<sub>4</sub>, CO<sub>2</sub>/N<sub>2</sub> Within a Charged Metal-Organic Framework

Lidan Kong, Ruyi Zou, Wenzhu Bi, Ruiqin Zhong, Weijun Mu, Jia Liu, Ray P.S. Han,  
Ruqiang Zou



A new ultramicroporous metal-organic framework with anionic framework and counter cations accommodated in the large channels is reported for CO<sub>2</sub> capture.